J Appl Electrochem (2008) 38:339–347
DOI 10.1007/s10800-007-9444-8

ORIGINAL PAPER

A thin-gap cell for selective oxidation of 4-methylanisole to 4-methoxy-benzaldehyde-dimethylacetal

Anis Attour · Sabine Rode · Athanassios Ziogas · Michael Matlosz · François Lapicque

Received: 21 July 2007 / Revised: 31 October 2007 / Accepted: 1 November 2007 / Published online: 24 November 2007

Abstract An electrochemical microreactor for organic electrosynthesis has been investigated for the anodic synthesis of 4-methylanisole to 4-methoxy-benzaldehyde-dimethylacetal in methanol solution. Selectivity and conversion in the single-pass thin-gap flow reactor were examined as a function of the composition of the electrolyte solution, the flow rate and the applied current. The experimental results indicate that potassium fluoride currently used for industrial synthesis and providing higher yields than sodium perchlorate, exerts an influence on the reaction mechanism: high KF concentrations facilitate the undesired oxidation of the diacetal. Nevertheless, a feed solution containing 0.1 M anisole in 0.01 M KF can be converted at 90% in the 100 μm thin-gap cell with acceptable voltages and a measured selectivity of nearly 87%. The selectivity observed substantially higher than that typically observed in conventional electrochemical cells.

Keywords Electroorganic synthesis · 4-methylanisole oxidation · Electrochemical microreactor · Supporting electrolyte · Process intensification

1 Introduction

Electroorganic synthesis is a domain in which microstructured devices are especially promising, with potential improvement of both production rates and selectivity. This study deals with design, construction and validation of a new microreactor for organic electrosynthesis. The model reaction is the anodic oxidation of 4-methylanisole (4-methoxy-toluene) to 4-methoxy-benzaldehyde-dimethylacetal. The reaction is important in industrial organic electrochemistry, due to the wide spread of the resulting aldehyde as a precursor and fragrance for fine chemicals production, including pharmaceuticals, dye-stuffs, plating additives, pesticides and flavour ingredients [1–4].

Because of poor space–time yields and considerable problems with work up and recycling of the electrolyte, indirect electrochemical processes have not been established industrially to date [5]. Hence, the direct oxidation of 4-methylanisole appears most promising for commercial production of benzaldehydes, and the reaction is performed by BASF with a production rate of 3,500 tons per year [2].

In methanol solution, the overall reaction of the electrochemical formation of anisaldehyde is described in Fig. 1 [6, 7]. The reaction mechanism consists of two distinctive steps: the electrochemical formation of the diacetal and the chemical hydrolysis to the respective aldehyde. A mechanism analogous to Fig. 2 has been proposed for the direct oxidation of toluenes in an alcohol solution [8–10].

The oxidation begins with an anodic electron transfer resulting in formation of a radical cation (step 1). This radical cation is stabilised in the methanol solvent by the formation of a benzylradical (step 2). Due to the lower oxidation potential of the benzylradical, it is transformed rapidly to a benzylcation (step 3). The benzylcation reacts with the methanol solvent (step 4), leading to the formation of the intermediate ether. The ether is then oxidised to the dimethylacetal by repeated electron transfers, stabilisation and addition of the methanol solvent (step 5). In the

A. Attour · S. Rode · M. Matlosz · F. Lapicque (✉)
Laboratoire des Sciences du Génie Chimique, CNRS-ENSIC, BP 20451, 54001 Nancy, France
e-mail: francois.lapicque@ensic.inpl-nancy.fr

A. Ziogas
Institut für Mikrotechnik Mainz (IMM) GmbH, Carl-Zeiss Strasse 18-20, 55129 Mainz, Germany

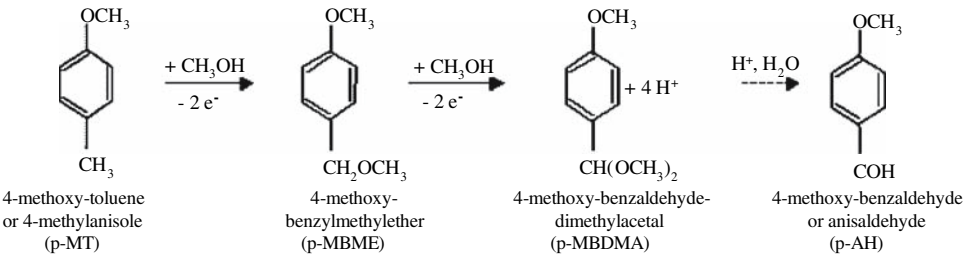

Fig. 1 Overall reaction for the electrochemical formation of 4-methoxy-benzaldehyde

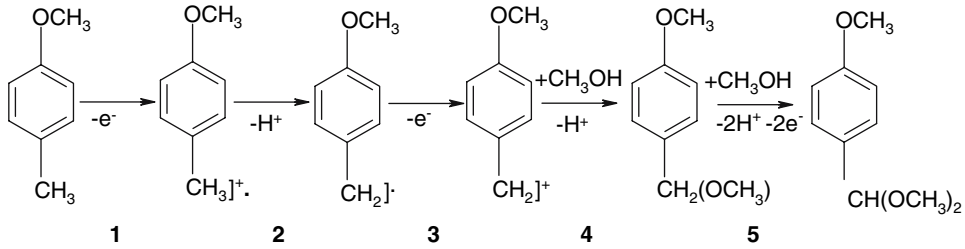

Fig. 2 Reaction sequence of anodic toluene oxidation in methanol

presence of water and in acidic media, the dimethylacetal undergoes hydrolysis which leads to the formation of 4-methoxybenzaldehyde (anisaldehyde) of commercial interest. In methanol, the reaction proceeds in a very rapid two-electron oxidation of the reagent to the benzylether followed by a subsequent rapid two-electron oxidation of the intermediate ether to the diacetal [8, 9]. The counter electrode (cathode) reaction is the reduction of methanol leading to hydrogen evolution (Fig. 1).

In parallel with the main reaction, side-reactions may also occur. Among these reactions, the following should be mentioned: (1) side oxidation of diacetal into 4-methoxy-trimethoxytoluene through further exchange of two electrons [8], (2) radical dimerisation and polymerisation reactions due to high concentration of protons and radicals, produced by step 2 especially at high current densities and reactant concentrations [9, 11], and (3) side addition of methanol to the benzene ring [9].

The oxidation reaction on carbon materials has been shown to be effective in methanol solution [2, 12, 13]. Kinetic constants of the successive formations of the ether, diacetal and ester—involving two electrons—have been determined on glassy carbon and on graphite surfaces [14].

Preparative oxidation of anisole has been carried out in conventional electrochemical cells [13, 14], or with the assistance ultrasonic generators [10], or in thin-gap cells such as the capillary-gap cell. The capillary-gap cell, with radial flow of electrolyte solution in the sub-millimetre gap formed by two neighbouring disk electrodes, has been patented by BASF for electroorganic synthesis [2, 15]. The cell is operated in a continuous mode and placed in a recycle loop. A process diagram including the separation steps can be found in [2]. High conversion of anisole has been shown with selectivity to diacetal/aldehyde of 68% [16]. More recently, Ziogas et al. [17] developed a thin-gap cell, with linear flow of the liquid in a 25 μm gap. In both thin gap cells, the high electrode area in comparison to the cell volume allows high conversion per pass. Moreover, mass transfer rates can be intensified in electrode gaps not significantly larger than the Nernst diffusion layer [18, 19], thereby improving the production rates and offering the possibility of single-pass electrochemical processes. Finally, thin electrode gaps result in reduced ohmic drops: lower amounts of supporting electrolyte can therefore be added to the solution, which simplifies the tedious separation of the product from the electrolyte solution downstream of the cell. Laboratory-scale studies have demonstrated the possibility of working without supporting electrolyte in thin-gap microreactors with satisfactory yields [20–22].

The present investigation is aimed at performing the anodic oxidation of anisole in a 100 μm thin-gap cell, based on the basis of the preliminary results obtained in previous work in a batch electrochemical cell [14]. The results presented in this work concern experimental investigations of the production of diacetal/aldehyde in order to determine the optimal operating conditions of the synthesis conducted in a the thin-gap flow cell operated in a single-pass continuous mode. For this purpose, the influence of the nature and concentration of the supporting electrolyte, the solution flow rate and the overall current has been emphasized. The goal of the work is to evaluate the amount of process intensification attained by the application of structured thin-gap microreactors in industrial production.

2 Materials and methods

2.1 Thin-gap microreactor

The thin-gap microreactor was an undivided flat electrode cell in PEEK (Polyetheretherketones) reactor housing. The PEEK housing was chosen for its excellent chemical and mechanical stability as well as good machinability [16, 17]. High-grade stainless steel was chosen as a cathode material. The anode was made of glassy carbon (Sigradur® HTW, Germany) providing suitable electrocatalytic properties and avoiding leakage of the electrolyte [14]. The anode consisted of ten 1 × 1 cm^2 elements, separated from each other by a 1 mm wide insulated section. The sealing was made of Chemraz®. In order to provide the required functionality, the cathode was first coated with approximately 50 µm Teflon® layer. The Teflon® layer was later removed by milling from the electrochemically active area. Special spring contacts (UWE Electronic) were employed and the rear side of the glassy carbon chips forming the anode was gold coated by sputtering in order to provide sufficient electrical contact and thus minimise the contact resistance. The two electrodes, with a 100 µm inter-electrode gap formed a 1 × 0.01 cm^2 channel cross sectional.

Construction of the cell was formed as follows: milling of the PEEK and of the high-grade stainless steel plate by a programmable CNC (Computer Numerically Controlled) machine; the glassy carbon plates as well as the Chemraz® sealing were cut by laser in order to provide the exact shape required and avoid any undesirable fracture of the material. The cell was produced at IMM (Institut für Microtechnik, Mainz, Germany) on the basis of the theoretical calculations published by Rode et al. [7].

A schematic view of the constructed cell is shown in Fig. 3. Although the anode was segmented, all carbon tiles were connected together for the experiments presented here, so that the cell voltage was uniform in the reactor.

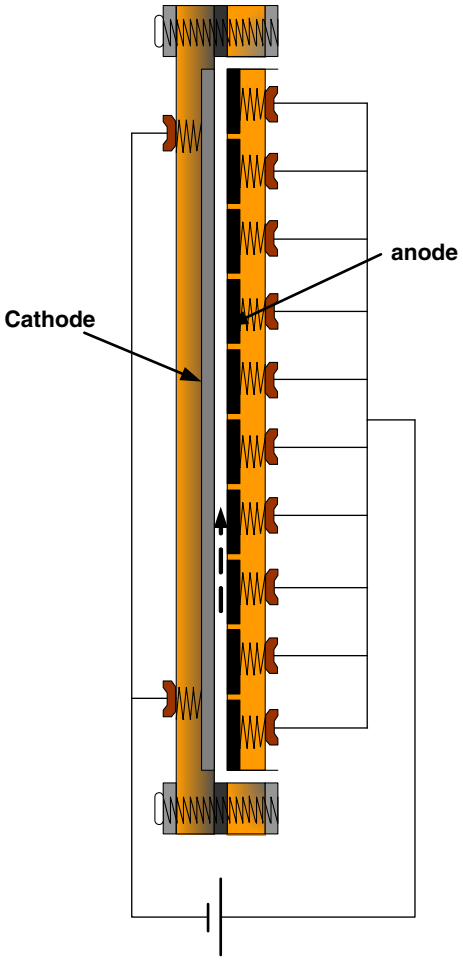

Fig. 3 Schematic view of the thin-gap cell

2.2 Experimental protocol

Experiments were conducted at ambient temperature, without cooling of the liquid or of the cell components. The overall current was applied to the cell either by a PGSTAT 10 potensiostat (Autolab).

In order to avoid the creation of gas plugs inside the microreactor, it is preferable that the flow of the electrolyte is upward (Fig. 3). The electrolytic solution was fed continuously to the cell by a syringe pump provided with two borosilicate glass syringes (Hamilton Company) of 100 cm^3 maximum volume. The syringe pump provide accurate feeds of 0.05–2 cm^3 min^{-1} to be injected. The corresponding velocity of the gas-free liquid ranged from 0.08 to 3.3 cm s^{-1}: the theoretical average residence time of the liquid calculated regardless of gas evolution, varied from 3 to 125 s. The cell was operated in single-pass mode, and the liquid leaving the cell was collected in glass tubes for further analysis. The time variations of the cell voltage were monitored using a data logger. Experiments showed that steady state of the cell was attained in a time ranging from 20 s to 3 min, depending on the liquid flow rate.

2.3 Chemicals and analytical procedure

The reactant, 4-methylanisole of purissimum grade, was purchased from Acros Organics. 4-Methoxy-benzaldehyde dimethyl acetal and 4-methoxy-benzaldehyde were Fluka puriss. products. For simplicity, the reactant and the two key products are denoted in this work as anisole, acetal and aldehyde. Methanol, from Merck, was of HPLC grade. Supporting electrolytes, namely sodium perchlorate and potassium fluoride, were of analytical grade and purchased from Acros Organics. The water content in the organic solutions was not determined.

However, preliminary tests were conducted with addition of orthoformic acid trimethylester for water removal, yielded similar results as other carried out without addition of the desiccation product in both RDE polarisation curves and reaction selectivity.

Analysis of the solution fractions collected at the outlet of the thin-gap microreactor was carried out by HPLC (Shimadzu) using an Inertsil ODS−3 250 × 4.6 mm column with an internal diameter of 5 μm and with a 55:45 acetonitrile-water eluent. Anisole, ether, acetal and aldehyde were detected at wavelength of 230 nm. Contrary to the other compounds, which could be purchased, the ether could not be directly calibrated, and the mole amount of the intermediate was estimated as follows:

For experimental conditions of cell operation leading to low/moderate conversion of the anisole, namely low applied currents, a peak located between those for the acetal and the aldehyde was identified. This peak increased with increasing anisole conversion, up to a limiting value. For higher conversions, i.e. for higher currents, the peak intensity declined and other peaks appeared in the chromatogram. The peak observed between those for the acetal and the aldehyde was therefore taken to correspond to the formation of the ether intermadiate. For low currents, for which no additional peaks were formed, a mass balance yielded the mole amount of ether, which was then correlated to the area of the corresponding peak. This indirect calibration was found to be of acceptable accuracy and the ether concentration could be estimated within 5%, whereas the accuracy was far better for anisole, acetal and aldehyde.

The other peaks in the chromatograms for higher currents could be partly identified by mass spectroscopy as triester, dimers and other side-products formed by addition of methanol to the benzene ring. In spite of their different chemical nature, these compounds have been considered here as a whole and referred as "secondary products". In particular analysis of oligomers was not specifically carried out. The significance of the secondary products was estimated by simple mass balance. Due to the method used, the accuracy in their determination could not be better than 10%.

The presence of aldehyde formed from acetal by hydrolysis was accounted for in the acetal mole number.

2.4 Parameters and variables

The dimensionless current was defined as the ratio of the overall current I passed to the minimum current required for total conversion of anisole to acetal with n_e= 4 electrons:

$$I^* = \frac{I}{n_e F Q_v C_{A,in}} \tag{1}$$

where Q_v is the volumetric flow rate of the solution and $C_{A,in}$ is the inlet concentration of anisole. I^* = 1 corresponds to 4 F/mol anisole. Anisole conversion was directly calculated from the concentration in the outlet liquid, $C_{A,out}$:

$$\theta = \frac{C_{A,in} - C_{A,out}}{C_{A,in}} \tag{2}$$

Reduced concentrations of intermediate ether (B) and acetal + aldehyde (C) were defined as follows:

$$C_B^* = C_{B,out}/C_{A,in} \tag{3a}$$

$$C_C^* = C_{C,out}/C_{A,in} \tag{3b}$$

Selectivity S for acetal-aldehyde was calculated as follows:

$$S = \frac{C_{C,out}}{(C_{A,in} - C_{A,out})} \tag{4}$$

The faradaic yield was defined on the basis of the formation of the key-product:

$$\Phi = \frac{n_e F Q_v C_{C,out}}{I} = \frac{C_c^*}{I^*} = \frac{S\theta}{I^*}. \tag{5}$$

3 Experimental oxidation of anisole

3.1 Selection of the supporting electrolyte

A preliminary series of experiments was carried out with anisole at 10^{-2} M in methanol solutions of sodium perchlorate at 0.4 M or potassium fluoride at 0.1 M, as studied previously with a stirred batch cell [14]. The flow rate was fixed at 0.6 cm^3 min^{-1}.

Anisole conversion in the thin-gap cell was followed as a function of dimensionless current I^*: no visible effect of the supporting electrolyte was observed (Fig. 4a). As expected, the conversion increased with I^*. For I^* larger than unity, the increase in conversion became much slower and θ attained 92% for the highest current tested, I^* = 1.6, corresponding to 6.4 F mol^{-1}.

The selectivity in acetal exhibited a maximum with I^*. This was expected since the key-product is not the final product of the three-step oxidation process. With the two supporting electrolytes, a well-defined maximum was observed for I^* near 0.8, i.e. 3.2 F mol^{-1} (Fig. 4b). Lower currents resulted in larger amounts of intermediate ether, whereas higher currents led to quantitative formation of side products, thereby affecting dramatically the selectivity. When sodium perchlorate was used, the selectivity did

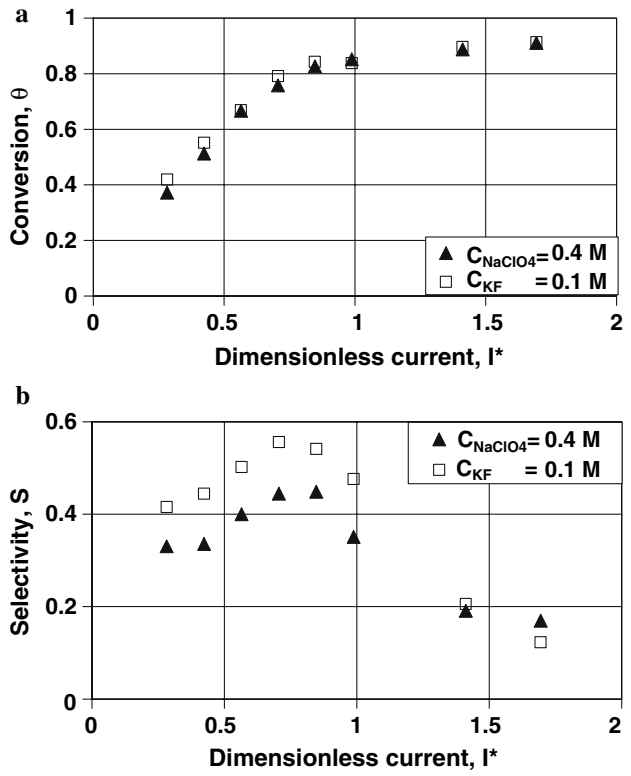

Fig. 4 Operation of the thin-gap cell with 0.01 M anisole in 0.4 M $NaClO_4$ or 0.1 M KF solutions fed at 0.6 cm^3 min^{-1}; (**a**) variation of the conversion with dimensionless current I^*; (**b**) variation of the selectivity for aldehyde/acetal with I^*

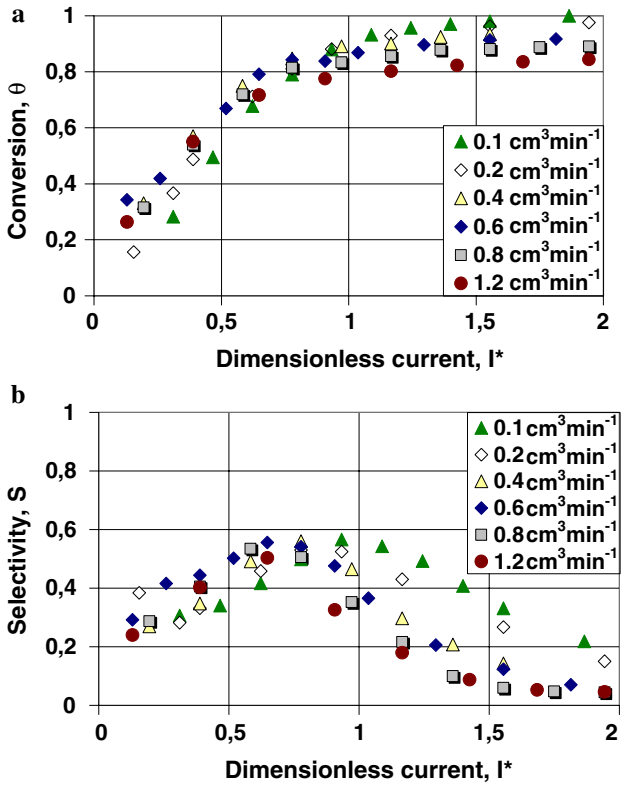

Fig. 5 Operation of the thin-gap cell with 0.01 M anisole in 0.1 M KF solutions as a function of flow rate in cm^3 min^{-1}; (**a**) variation of the conversion with dimensionless current I^*; (**b**) variation of the selectivity for aldehyde/acetal with I^*

not exceed 45%. This corroborates the previous measurements done in a stirred discontinuous cell [14]. The corresponding faradaic yield reached 48% for the optimal values of the current density (data not shown). As observed previously with the batch cell, potassium fluoride allowed higher selectivity, up to 55% under the above operating conditions (Fig. 4b), corresponding to a maximum faradaic yield of 58%. Potassium fluoride was then employed for all further experiments.

3.2 Effect of the solution flow rate with low anisole concentration

The anisole concentration was initially fixed at 0.01 M and the flow rate varied from 0.05 to 1.2 cm^3 min^{-1}; for $I^* = 1$, the corresponding current ranged from 0.006 to 0.08 A. The anisole conversion increased linearly with I^* for low values of the dimensionless current (Fig. 5a). Such a variation corresponds to a zero-order reaction in the cell, and this behaviour can be expected for cases in which the local current density is below the limiting current density throughout the cell [23, 24]. The slope of the linear variation provides an indication of the number of electrons effectively consumed per converted anisole molecule, n_{eff}, introduced in a previous paper [14]. From the expression of I^*, the slope can be expressed as:

$$\left(\mathrm{d}\theta/\mathrm{d}I^*\right)_{I^*=0} = \frac{n_e}{n_{eff}} \tag{6}$$

The slope, estimated at 1.2, corresponds to a n_{eff} of approximately 3.3: the difference between n_{eff} and its theoretical value $n_e = 4$ can be attributed to formation of dimers and intermediate ether. The n_{eff} value is somewhat larger than that obtained with the batch cell [14], suggesting that smaller amounts of dimers and ether were produced in the thin-gap cell in comparison with the batch cell. For dimensionless currents greater than 1–1.5, the conversion attained a plateau, the level of which depended on the flow rate. Total conversion was attained for the lowest flow rates, whereas the plateau did not exceed 84% at 1.2 cm^3 min^{-1}: for such conditions anisole conversion appeared to be partly diffusion-controlled.

The selectivity to the key-product exhibited a maximum of around 50% for dimensionless currents near one (Fig. 5b). The location of the maximum depended nevertheless on the flow rate, decreasing from 1 at the lowest

flow rate to approximately 0.7 at 1.2 cm^3 min^{-1}. Low currents do not allow sufficient conversion of intermediate ether to diacetal; conversely, dimensionless currents far above unity result in further oxidation to the ester. Mass balances at the current corresponding to maximum selectivity indicated that nearly 25% of inlet anisole was converted to "secondary" products, with little influence of the flow rate.

3.3 Effect of the solution flow rate with more concentrated media

In order to investigate the electrochemical reaction in conditions more representative of industrial practice, the anisole concentration in the feed was increased to 0.1 M. Concentrations greater than 0.1 M were not investigated in order to avoid excessive currents in the cell and extensive gas evolution, which could result in significant ohmic drops and heat production in the small cell, with possible vaporisation of the methanol near the electrode surface, as shown by heat transfer simulations [25].

For the same variation of the flow rate as in Section 3.2, the current ranged from 0.033 to 0.8 A. Applying Faraday's law to the cathode for $I^* = 1$ yields hydrogen flow rates at ambient temperature and pressure approximately five times larger than that of the liquid phase. Regardless of the rate of the liquid feed, the hydrodynamics were substantially modified by the gas evolution in the thin gap channel and slug flow of the two phases was usually observed in the outlet tube. The cell voltage varied from 2.7 to 5.8 V depending on both I^* and the solution flow rate (Fig. 6). The cell voltage measured after opening the electrical circuit was near 1.9 V, far below the above voltage values. Although the overpotential of hydrogen evolution at the stainless-steel cathode cannot be estimated easily, a comparison of the voltages at zero current and during production tests suggested a significant ohmic drop in the cell. Taking into account the conductivity of the solution, measured to be 0.45 S m^{-1} at ambient temperature, and the electrode gap, the ohmic drop in the gas-free liquid section was estimated at 0.027 V for $I^* = 1$ and at 0.2 cm^3 min^{-1}, which is likely to be far below the actual ohmic drop through the two-phase medium.

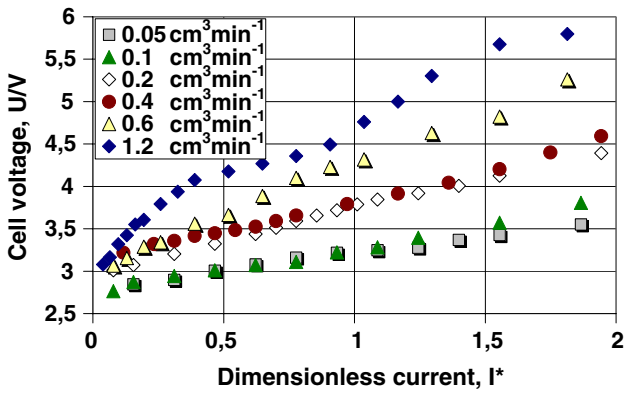

Fig. 6 Operation of the thin-gap cell with 0.1 M anisole in 0.1 M KF solutions as a function of flow rate in cm^3 min^{-1}: variation of the cell voltage with dimensionless current I^*

Anisole conversion increased linearly with the dimensionless current (Fig. 7a) for I^* below 0.7, regardless of the flow rate. Interpretation of the linear part of the variation yielded an effective number of exchanged electrons of 3 within 10%. Contrary to what was observed with diluted anisole media, anisole could be totally converted for I^* larger than approximately 1.5, indicating that the reaction pathway depends also on the relative importance of the reactant concentration in comparison to that of the solvent phase. Moreover higher transfer rates may be expected in concentrated media. The reduced concentration of ether, C_B^*, exhibited an expected maximum (Fig. 7b), whose location and intensity nevertheless depended strongly on the flow rate. The largest flow rates did not allow substantial amounts of ether whose reduced concentration was below 15% for I^* near 0.3. Reducing the flow rate resulted in a shifted maximum of C_B^* toward higher I^* values and the reduced concentration of ether could attain 30%. Moreover, the selectivity profile was affected by the solution flow rate as shown in Fig. 7c. The location of the maximum was shifted toward higher I^* values by reduction of the flow rate: for the lowest flow rate, selectivity up to 70% could be obtained for I^* near unity, whereas a flat maximum near 50% was observed for I^* around 0.8 for the highest flow rate.

Low flow rates of the reactant solution appear favourable for the selectivity of the synthesis but are detrimental to the production rate in the reactor. As a result, a compromise must be found for optimal production.

3.4 Effect of the concentration of supporting electrolyte

Electrochemical synthesis at the lab scale is often investigated with high concentrations of supporting electrolyte, which is assumed to be inert chemically and electrochemically, in order to reduce ohmic drops between the working electrode and the reference. For preparative electrosynthesis, high concentrations of supporting electrolyte give rise to additional issues that must be examined: (1) cost of the electrolyte, (2) chemical/electrochemical inertia of the supporting electrolyte, and (3) separation of the key product from the electrolytic solution and recovery of the salt. As a result, lower concentrations of supporting electrolyte may be preferred in industrial practice.

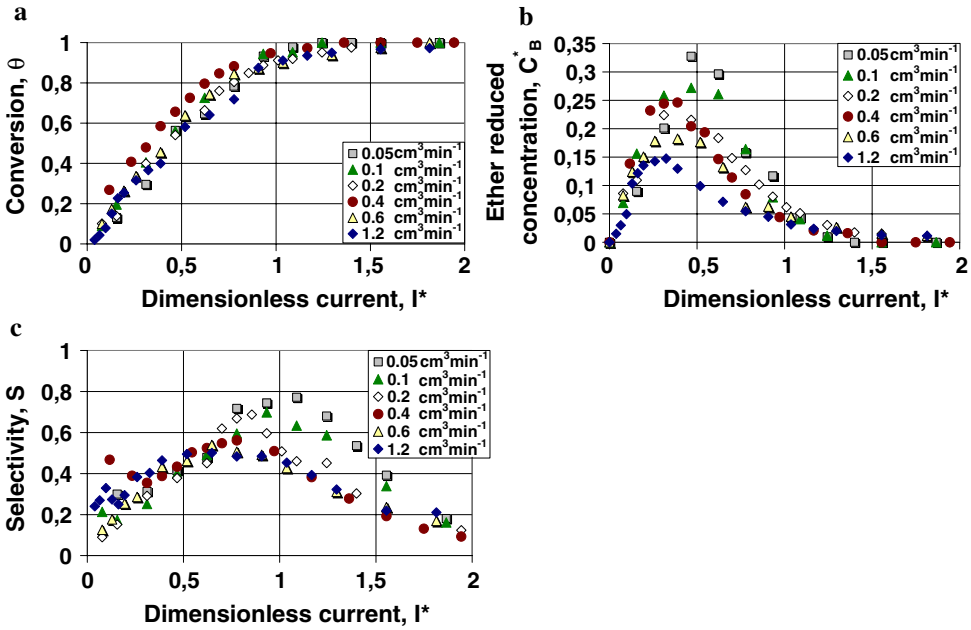

Fig. 7 Operation of the thin-gap cell with 0.1 M anisole in 0.1 M KF as a function of flow rate in $cm^3\ min^{-1}$; (**a**) variation of the conversion with dimensionless current I^*; (**b**) variation of the reduced concentration of ether, C_b^*, with I^*; (**c**) variation of the selectivity for aldehyde/acetal with I^*

To study the influence of supporting electrolyte, the flow rate was fixed at 0.2 $cm^3\ min^{-1}$, allowing high selectivity of the acetal synthesis and reasonable production rate of the thin-gap cell. The anisole conversion was not affected by a KF concentration (Fig. 8a). The selectivity and the faradaic yield were shown to be enhanced by a reduction in KF concentration, which was reduced to 0.0025 M, i.e. 145 mg L^{-1}. For the flow rate considered, both the selectivity and the faradaic yield exhibited a maximum for I^* near 0.85, corresponding to a current of 0.12 A. The maximum selectivity varied from 65% with 0.1 M KF to 87% for KF concentrations at 0.005 or 0.01 M (Fig. 8b). Very similar figures of the faradaic yield were obtained: 72% with 0.1 M KF and 94% with 0.01 M (Fig. 8c). This result clearly shows that the supporting electrolyte cannot be considered as perfectly inert, although it is currently used industrially for this synthesis [2, 13, 17]. However, the experimental observation could not be supported by a detailed mechanism of the precise role of potassium fluoride. The dimensionless concentration of secondary products, $C^*_{sec.pr.}$, was observed to increase with I^* (Fig. 8 d), due to more significant oxidation of acetal to ester, and possibly more significant formation of dimers. Nevertheless, reducing the concentration of supporting electrolyte to

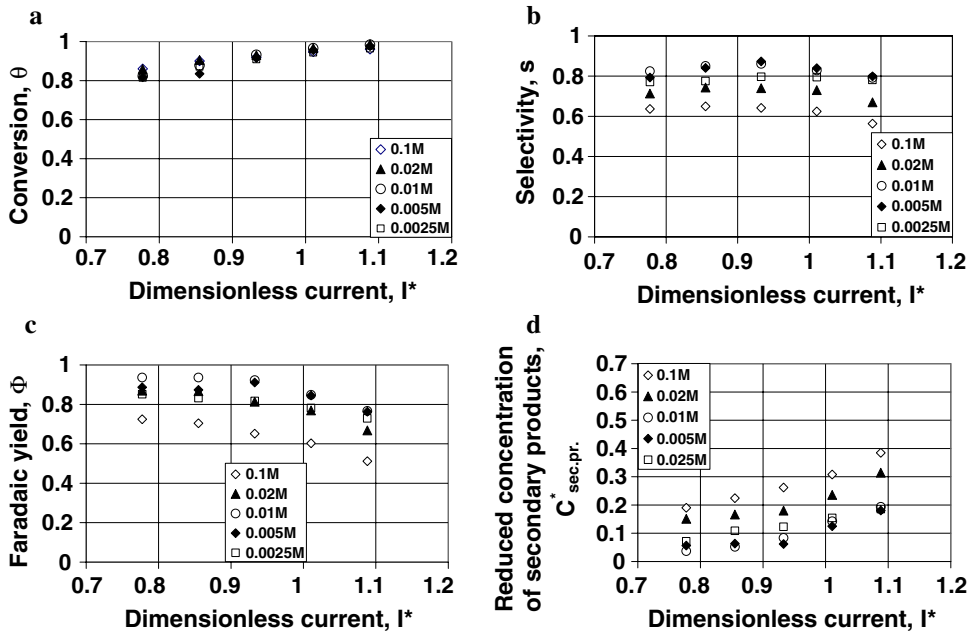

Fig. 8 Operation of the thin-gap cell with 0.1 M anisole in methanol with various concentrations of KF, at 0.2 $cm^3\ min^{-1}$; (**a**) variation of the conversion with dimensionless current I^*; (**b**) variation of the selectivity for aldehyde/acetal with I^*; (**c**) variation of the faradaic yield; (**d**) variation of the reduced concentration of secondary product, $C^*_{sec.pr.}$, with I^*

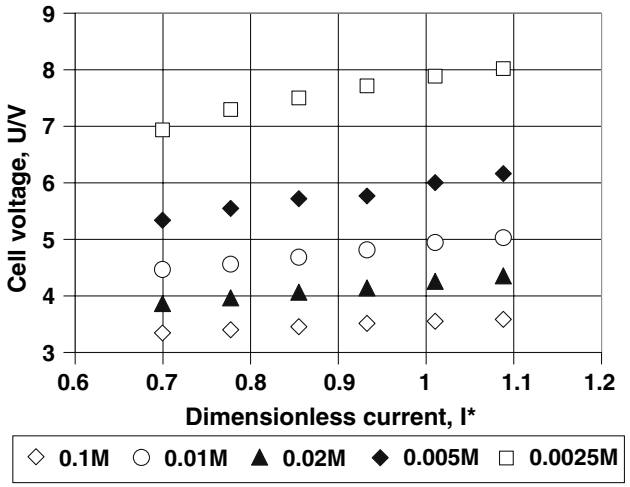

Fig. 9 Operation of the thin-gap cell with 0.1 M anisole in methanol with various concentrations of KF, at 0.2 cm^3 min^{-1}: cell voltage vs. dimensionless current I^*

0.01 M or below resulted in a significant reduction in the secondary products formed, corresponding to the high selectivity mentioned.

The side-effect of lower concentrations of supporting electrolyte is the dramatic rise of the cell voltage, increasing from 3.5 V with 0.1 M KF to 7.8 V in the most dilute solution (Fig. 9). KF at 0.01 M appears a good compromise for very high selectivity and acceptable cell voltage, in the range 4.6–4.9 V depending on I^* in the vicinity of the optimal applied current. Taking into account the conductivity of the 0.01 M KF solution, 0.053 S m^{-1}, at ambient temperature, and the electrode gap, the ohmic drop in the gas-free liquid section can be estimated at approximately 0.24 V for $I^* = 1$. As mentioned above, the actual ohmic drop in the cell is likely to be far above this value due to the high volume fraction of the gas phase.

The thin-gap cell operated with a 0.2 cm^3 min^{-1} solution containing 0.1 M anisole and 0.01 M KF allows nearly total conversion of the reactant with selectivity over 85%, compared with the selectivity obtained in the industrial cell with recirculation of electrolyte at 68% [15, 17].

4 Conclusion

The efficiency of a thin-gap cell for the electrosynthesis without recirculation of the electrolyte solution has been demonstrated here for the anodic oxidation of 4-methyl-anisole to 4-methoxy-benzaldehyde-dimethylacetal. The miniaturised cell allows substantial reduction of supporting electrolyte with acceptable ohmic drops. The supporting electrolyte used in this work as well as for industrial practice has been shown to play a role in the synthesis: higher concentrations of potassium fluoride were shown to favour the oxidation of the key product to ester. In spite of substantial ohmic drops in the 100 μm thin-gap cell, electroynthesis can be efficiently carried out with 0.01 M potassium fluoride: total conversion and selectivity over 85% could be obtained.

More concentrated reagent solutions could be treated in systems with integrated heat exchange. Heat exchanger would avoid overheating of the cell components and of the electrolytic media in these systems for which intensification and very high production rates are accompanied by significant heat generation due to irreversibility and ohmic drop. In addition, working at pressures far above the atmospheric pressure is envisioned to reduce void fractions in the electrode gap, ease removal of hydrogen bubbles, and minimise ohmic drops.

Acknowledgments Financial support for this work was provided by the European Project Impulse (project reference ID NMP2-CT-2005-011816 of the 6th Framework Programme for Research and Technological Development of the European Union). The authors also thank the French Ministry of Research for the PhD grant allocated to A. Attour.

References

1. Bersier BM, Carlsson L, Bersier J (1994) Topics in current chemistry. Springer-Verlag, Berlin, Heidelberg
2. Lund H, Hammerich O (2001) Organic electrochemistry, 4th edn. Marcel Dekker, New York
3. Pletcher D, Walsh FC (1990) Industrial electrochemistry, 2nd edn. Chapman-Hall, London–New York, 1990
4. Nishiguchi I, Hirashima T (1985) J Org Chem 50:539
5. Degner D (1988) Organic electrochemistry in industry. In: Topics in current chemistry. Springer-Verlag, Berlin, Heidelberg
6. Löwe H, Ehrfeld W (1999) Electrochim Acta 44:3679
7. Rode S, Altmeyer S, Matlosz M (2004) J Appl Electrochem 34:671
8. Wendt H, Bitterlich S (1992) Electrochim Acta 37:1951
9. Wendt H, Bitterlich S, Lodowicks E, Liu Z (1992) Electrochim Acta 37:1959
10. Lindermeir A, Horst C, Hoffmann U (2003) Ultrasonics Sonochem 10:223
11. Bitterlich S (1990) PhD thesis, TH Darmstadt
12. Venkatachalapathy MS, Ramaswamy R, Udupa HVK (1958) Bull Acad Polon Sci Ser Sci Chim 6:478
13. Wendt H, Schneider H (1986) J Appl Electrochem 16:134
14. Attour A, Rode S, Bystron T, Matlosz M, Lapicque F (2007) J Appl Electrochem 37:861
15. Beck F (1987) Organic electrosynthesis, Ullmann's encyclopedia of industrial chemistry. VCH Verlagsgesellschaft mbH, Weinheim
16. Küpper M, Hessel V, Löwe H, Stark W, Jinkel J, Michel M, Schmidt-Traub H (2003) Electrochim Acta 48:2889
17. Ziogas A, Löwe H, Küpper M, Ehrfeld W (2000) Electrochemical microreactors: a new approach for microreaction technology. In: Ehrfeld W (ed) Microreaction technology: industrial prospects, IMRET3: Proceedings of the 3rd international conference on

microreaction technology, Frankfurt/Main. Springer-Verlag, Berlin, pp 136–156
18. Cao E, Gavridilis A, Motherwell WB (2004) Chem Eng Sci 59:4803
19. Ge H, Chen G, Yuan Q, Li H (2005) Catalysis Today 110:171
20. Paddon CA, Pritchard GJ, Thiemann T, Marken F (2002) Electrochem Commun 4:825
21. Horri D, Atobe M, Fuchigami T, Marken F (2005) Electrochem Commun 7:35
22. He P, Watts P, Maken F, Haswell SJ (2005) Electrochem Commun 7:918
23. Goodridge F, Scott K (1995) Electrochemical process engineering. Plenum Press, New York and London
24. Pickett DJ (1979) Electrochemical reactor design, 2nd edn. Elsevier, New York, 1979
25. Attour A (2007) Réacteur d'électrosynthèse microstructuré: conception, étude et développement appliqués à l'oxydation du 4-méthylanisole, PhD Dissertation, INPL, Nancy (in French)